Check for updates

GDCh Research Article Angewandte International Edition Chemie www.angewandte.org

How to cite: *Angew. Chem. Int. Ed.* **2024**, *63*, e202412534
doi.org/10.1002/anie.202412534

Synthetic Biology

Regulating Nucleic Acid Catalysis Using Active Droplets

Anna-Lena Holtmannspötter[+], Corbin Machatzke[+], Christian Begemann, Elia Salibi, Carsten Donau, Fabian Späth, Job Boekhoven, and Hannes Mutschler**

Abstract: Cells use transient membraneless organelles to regulate biological reaction networks. For example, stress granules selectively store mRNA to downregulate protein expression in response to heat or oxidative stress. Models mimicking this active behavior should be established to better understand in vivo regulation involving compartmentalization. Here we use active, complex coacervate droplets as a model for membraneless organelles to spatiotemporally control the activity of a catalytic DNA (DNAzyme). Upon partitioning into these peptide-RNA droplets, the DNAzyme unfolds and loses its ability to catalyze the cleavage of a nucleic acid strand. We can transiently pause the DNAzyme activity upon inducing droplet formation with fuel. After fuel consumption, the DNAzyme activity autonomously restarts. We envision this system could be used to up and downregulate multiple reactions in a network, helping understand the complexity of a cell's pathways. By creating a network where the DNAzyme could reciprocally regulate the droplet properties, we would have a powerful tool for engineering synthetic cells.

Introduction

Membraneless compartmentalization is a key element of cellular organization[1] and offers a tool to spatially and temporally separate reaction pathways in its complex reaction networks.[1b,2] Typically, these membraneless organelles comprise RNA and intrinsically disordered proteins held together by entropic effects and electrostatic interactions.[3] Spatial separation through membraneless organelles can occur in response to an external trigger such as stress, resulting in the selective removal of specific RNA, thereby stopping the transcription of those and the activity of their encoded downstream proteins.[4]

Model systems of these biological condensates help us to understand the complexity of such chemical reaction networks. One of such models are the droplets formed by complex coacervates—a type of liquid phase separation typically composed of oppositely charged polyions.[5] Several studies on coacervates in combination with reaction cycles and biocatalysts like enzymes, ribozymes, or DNAzymes exist to test how droplets regulate chemical activity.[6] Most of these studies focused on enhancing reaction rates by coacervation, but some inhibitory systems were also described.[7] Transient inhibition, as seen in stress granules, has not yet been achieved. Given the non-equilibrium nature of the cell, most membraneless organelles are also active and transient.[1a,8] However, the models combining coacervates and biocatalysts typically operate close to equilibrium, lacking this active aspect of membraneless organelles.

Inspired by the active environment of the cell, chemically fueled, active droplets have been developed (Scheme 1A).[9] In these systems, a (photo-) chemical reaction cycle regulates the ability of building blocks to phase-separate.[10] Specifically, a molecule with high chemical potential ("fuel") reacts with the building blocks, which activates them for phase separation ("activation"). A spontaneous back-reaction reverts the activated building block to its initial state ("deactivation"). This means that when building blocks are supplied with fuel, a population of transiently activated building blocks emerges, resulting in active droplets. Moreover, when a finite amount of fuel is supplied, the system will temporarily produce droplets until all fuel is consumed.

Such active droplets are a class of chemically fueled assemblies,[11] and their fuel-dependent nature makes them an ideal model to test how transient compartmentalization affects biocatalysts in reaction networks. In this context, active assemblies have been used to host and modulate reactions and model complex biological systems. For example, chemical fuels have been used to generate vesicles, which locally increase the concentration of hydrophobic reagents, thereby increasing the rate of a Diels-Alder reaction.[12] Alternatively, vesicle formation that contains DNA cargo is transiently controlled by UV light, mimicking the formation of membraneless organelles. Other works tackle the impact of non-equilibrium systems on catalytic activity using agarose gel-based systems.[13] However, active coacervate droplets that control chemical reactions have yet

[*] A.-L. Holtmannspötter,[+] C. Donau, F. Späth, J. Boekhoven
Department of Bioscience, School of Natural Sciences, Technical University of Munich, Lichtenbergstrasse 4, 85748 Garching, Germany
E-mail: job.boekhoven@tum.de

C. Machatzke,[+] C. Begemann, E. Salibi, H. Mutschler
Department of Chemistry and Chemical Biology, TU Dortmund University, Otto-Hahn-Strasse 4a, 44227 Dortmund, Germany
E-mail: hannes.mutschler@tu-dortmund.de

[+] These authors contributed equally to this work.

© 2024 The Authors. Angewandte Chemie International Edition published by Wiley-VCH GmbH. This is an open access article under the terms of the Creative Commons Attribution License, which permits use, distribution and reproduction in any medium, provided the original work is properly cited.

© 2024 The Authors. Angewandte Chemie International Edition published by Wiley-VCH GmbH

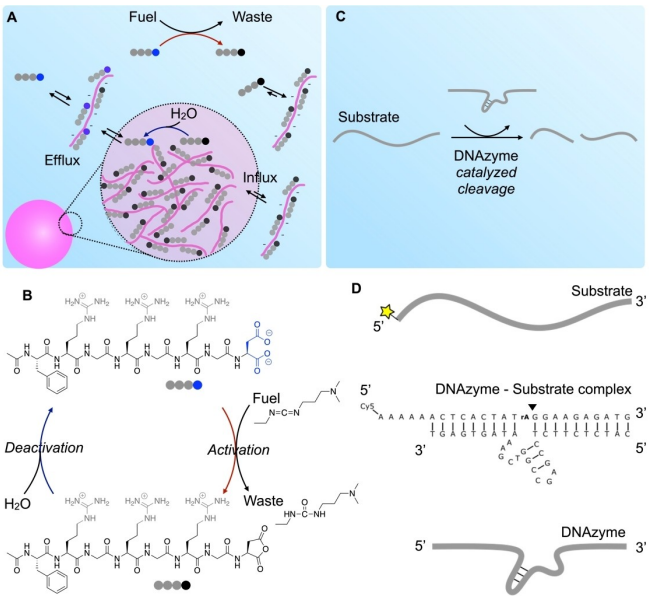

Scheme 1. The active coacervate droplet system and DNAzyme-catalyzed reaction. **A**. The assembly of peptides (beads) and RNA (pink strands) into active coacervate droplets is regulated by a fueled cycle. **B**. The peptide (blue bead) is activated by a carbodiimide fuel, increasing the net charge from +1 to +3 by forming an anhydride. This increases its affinity for the negatively charged RNA. The activated peptide (black bead) spontaneously deactivates back to its original form by hydrolysis. **C**. The DNAzyme catalyzes the cleavage reaction of a substrate strand. **D**. The sequence of the DNAzyme and its substrate. The substrate comprises all DNA but one RNA base at the cleavage site.

to be studied despite their potential as a model for membraneless organelles.

In this work, we test how a dynamic environment of active droplets can regulate the activity of a biocatalyst, specifically DNAzymes. DNAzymes are catalytically active DNA oligomers and a versatile model for biocatalytic reactions due to their robustness and stability compared to catalytic RNAs or enzymes.[14] As no naturally occurring DNAzymes exist, all known ones were isolated during in vitro selection experiments.[15] We spatio-temporally control the catalytic activity of a short DNAzyme using active droplets. These active droplets emerge and decay in the presence of fuel. Upon partitioning in the active droplets, the DNAzyme unfolds and loses its ability to catalyze the cleavage of an RNA substrate. By adding fuel, we reversibly halt the DNAzyme activity by temporal partitioning into the droplets. Moreover, we show that this "on-and-off" activity can be repeated multiple times. We envision that such a system could create reaction networks that rely on the spatiotemporal separation and inactivation of catalyst and substrate.

Results and Discussion

System Design and DNAzyme Partitioning

The active droplets are based on a complex coacervate between a long RNA polyanion (polyU, 2200 monomer units) and a short cationic peptide (Scheme 1A).[9a] The formation of droplets is regulated by a chemical reaction cycle that consumes EDC as a chemical fuel.[16] Specifically, the C-terminus of peptide (Ac-F(RG)$_3$D-OH) reacts with the fuel, resulting in its corresponding anhydride (Activation, Scheme 1B). This activation increases the overall charge of the peptide from +1 to +3. The anhydride spontaneously hydrolyzes to the original peptide (Deactivation, Scheme 1B). Because of its overall charge, the peptide cannot form coacervates. However, the transient increase in charge enables the activated peptide to form complex coacervate-based droplets. Thus, when a batch of fuel is added, the chemical reaction cycle consumes it, leading to a population of transiently activated peptides that form droplets until the fuel runs out. We combined these droplets with the 17E DNAzyme—a zinc-dependent catalyst that catalyzes site-specific RNA cleavage via transesterification (Scheme 1C).[17] We used a substrate composed of DNA, except at the cleavage site, where the presence of a 2'-OH of RNA is needed for cleavage (Scheme 1D).

For the droplets to exert control over the DNAzyme, the DNA has to partition in the droplets which we first tested (Figure 1A–D). Unless stated otherwise, we made droplets using 23 mM peptide, 4.1 mM polyU (expressed as the monomer concentration) tagged with 200 nM A_{15}-Cy5 RNA for imaging, 40 mM fuel, 1 mM $ZnCl_2$, 200 nM DNAzyme tagged with Cy3 for imaging, and 200 mM MES buffer (pH 5.3). We imaged the droplets after 5 minutes using a confocal microscope (Figure 1B, Figure S1). We observed poor colocalization between the droplet-forming polyU and the DNAzyme, likely due to the short length and the secondary structure of the DNAzyme.

To increase the partitioning of the DNAzyme into the droplets, we added an A_{10} "partitioning arm" to each end of the DNAzyme (DNAzyme-A10). We hypothesized that the adenines pair with the polyU RNA inside the droplets (Figure 1A), thereby facilitating partitioning. Indeed, DNAzyme-A10 showed strong colocalization with the tagged polyU upon fuel-induced droplet formation (Figure 1C), which we quantified by measuring the fluorescence intensity of multiple regions of interest (ROIs) inside of the droplets as a measure for the concentration of DNAzyme inside the droplets. After pelleting the droplets by centrifugation, we recorded micrographs of the supernatant and determined their intensity as a measure of the DNAzyme concentrations in the bulk phase. We calculated the partition coefficient (K_P) from this data, which represents the ratio between the concentration inside the droplets and in the supernatant. Similarly, we determined the K_P of the DNAzyme-A10, the substrate, and the product of the reaction (Figure 1D). As expected, the A_{10} partitioning arms significantly increased the partitioning of the DNAzyme, achieving more than a 300-fold enhancement ($K_P = 8600 \pm 500$). In contrast, the

© 2024 The Authors. Angewandte Chemie International Edition published by Wiley-VCH GmbH

15213773, 2024, 47, Downloaded from https://onlinelibrary.wiley.com/doi/10.1002/anie.202412534, Wiley Online Library on [14/11/2024]. See the Terms and Conditions (https://onlinelibrary.wiley.com/terms-and-conditions) on Wiley Online Library for rules of use; OA articles are governed by the applicable Creative Commons License

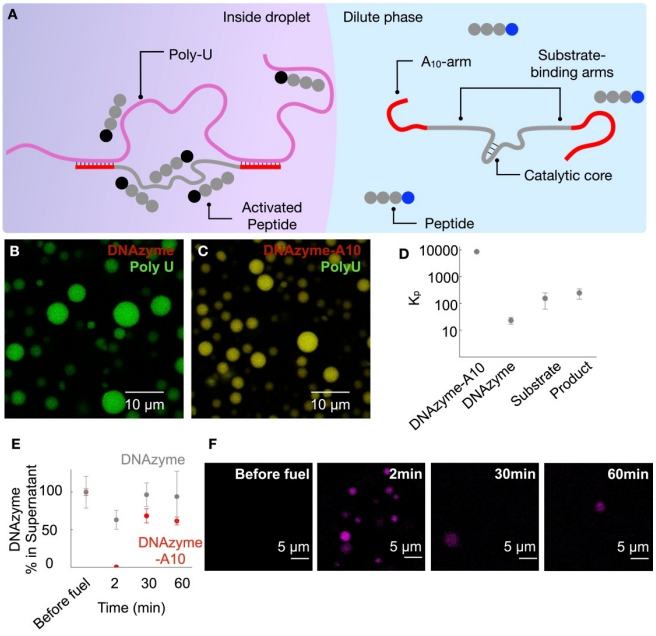

Figure 1. The molecular design of a DNAzyme controls its partitioning in transient droplets. **A**. Schematic representation of the modified DNAzyme inside and outside of the droplet. **B–C**. Confocal micrographs of a solution of complex coacervate droplets 5 minutes after fuel addition stained with a DNAzyme (Cy3, red) and a short RNA oligomer A_{15}, complementary to the poly U (A_{15}-Cy5, green). The DNAzyme with two terminal A10 arms (DNAzyme-A10) partitions preferentially inside of the droplets, whereas the DNAzyme without does not. **D**. The partition coefficients K_p of the DNAzyme, substrate, and product as calculated from the micrographs. K_p is the ratio between the concentration inside the droplets and in the supernatant. A more detailed definition can be found in the Methods section of the SI. The error bars correspond to the standard deviation of three replicates; if none are visible, they are smaller than the size of the data point. **E**. The percentage of DNAzyme and DNAzyme-A10 in the supernatant at different times after fuel addition as measured by PAGE. The error bars correspond to the standard deviation of three replicates; if none are visible, they are smaller than the size of the data point. **F**. Confocal micrographs of a solution of complex coacervate droplets 2 minutes, 30 minutes, and 60 minutes after adding fuel, stained with the Cy3-dye labeled DNAzyme-A10.

substrate ($K_P = 150 \pm 90$) and product ($K_P = 200 \pm 100$) partition inside the droplets to a lesser degree than the modified DNAzyme. No cooperative effect was observed in the partitioning of the substrate or product with DNAzyme-A_{10}. The K_P of the substrate and product remain consistent regardless of the presence of DNAzyme-A10. (Figure S8)

Next, we calculated the fraction of DNAzyme partitioned into the droplets after fuel addition (see Supporting Note 1). We determined the droplet volume of all combined droplets in a (73.81 µm×73.81 µm×10 µm) box by confocal microscopy. Five minutes after fuel addition, the droplets accounted for 0.6 % of the total volume. Combining this data with the partition coefficients, we calculated the percentage of DNAzyme outside the droplets to be 2 % for DNAzyme-A10 and 88 % for the unmodified DNAzyme. In comparison, approximately half of the substrate remained outside of the droplets (52 %). This finding demonstrates no significant separation of the catalyst and substrate for both DNAzymes, particularly given the considerable material exchange between droplets and supernatant.

The partitioning data was further confirmed with an orthogonal method based on gel electrophoresis (Figure S2). We prepared droplets with 1 µM DNAzyme-A10 and substrate and took samples before fuel addition. After the droplet formation, we separated them from the supernatant by centrifugation. We separated the DNA species in the pellet and supernatant using polyacrylamide gel electrophoresis (PAGE) and quantified them with fluorescent gel imaging. This method confirmed that 1.5 % of the DNAzyme-A10 is present in the supernatant. This result and the confocal data support that most DNAzyme-A10 partitions into the droplets.

Given the fuel-dependent nature of droplet formation, we expect a release of the DNAzyme after the fuel depletion. Using a previously described kinetic model,[9a] we predicted that the system consumed the fuel in roughly 30 minutes and that, during the cycle, a maximum concentration of 4.4 mM of activated peptide was reached after 2 minutes. The model predicts that after 30 minutes, most of the activated peptide had been deactivated. Therefore, we used the same gel-based method described above to determine the release of the DNAzyme into the supernatant. Surprisingly, we measured a release of only 67 % of DNAzyme-A10 30 minutes after fuel addition (Figure 1E). Moreover, this value did not increase further after 60 minutes. By analyzing the samples using confocal microscopy, we observed that the droplets had not completely dissolved 60 minutes after the addition of the fuel (Figure 1F). Thus, the apparent time delay between fuel consumption and droplet dissolution might explain why the DNAzyme-A10 is not completely released into the solution. Indeed, when we determined the volume of the droplets by confocal microscopy at 30 and 60 minutes, we found it had reduced from 0.6 % after five minutes to 0.2 % at both of those time points (Figure S4). In other words, only two-thirds of the droplet material had dissolved up to 60 minutes after fuel addition, which is in line with only two-thirds of the polyU-bound DNAzyme-A10 being released. In contrast, the unmodified DNAzyme did not partition well into the droplets after two minutes and was mostly released after 30 minutes (Figure 1E).

We suspected the millimolar amounts of Zn^{2+} ions to be responsible for the incomplete dissolution of the droplets. Measuring turbidity traces as a proxy for the presence of droplets, we found that in the absence of $ZnCl_2$, the droplets dissolved after 22 minutes. In contrast, with 1 mM $ZnCl_2$, we found that the turbidity decreased but did not completely disappear (Figure S3). Potentially, a change in the polyanion could optimize our system and solve the inability to dissolve in the future. We attempted to form droplets with our peptide, fuel, and polyT DNA (80mers) or genomic ssDNA as polyanions as a first test (Figure S15). Droplets formed only at very high fuel concentrations, or we observed the formation of non-dissolving aggregates, leading us to continue with the polyU-based system. In summary, we can

© 2024 The Authors. Angewandte Chemie International Edition published by Wiley-VCH GmbH

15213773, 2024, 47, Downloaded from https://onlinelibrary.wiley.com/doi/10.1002/anie.202412534, Wiley Online Library on [14/11/2024]. See the Terms and Conditions (https://onlinelibrary.wiley.com/terms-and-conditions) on Wiley Online Library for rules of use; OA articles are governed by the applicable Creative Commons License

control the partitioning of a modified DNAzyme by the fuel-induced presence of active droplets.

Compatibility of the DNAzyme with Active Droplets

Next, we investigated the DNAzyme activity in the presence of droplets. Using gel electrophoresis, we tracked the reaction catalyzed by the modified and unmodified DNAzyme in the absence and presence of droplets (Figure 2A, Figure S9). For these activity measurements, we used 1 μM of DNAzyme or DNAzyme-A10, 4 μM of substrate-Cy5, 2 mM $ZnCl_2$, and the same peptide, polyU, and buffer concentrations as described above. To ensure the sustained presence of droplets, we fueled the solution with 10 mM EDC every 5 minutes for 45 minutes.

Both DNAzymes converted 94 % of the substrate over 3 hours at the same rate, showing that the A10 modifications did not affect activity. In contrast, the presence of droplets drastically decreased the yield after three hours to only 14 % for the DNAzyme-A10. For the unmodified DNAzyme, the decrease was only 48 %. We explain the drop in yield by the high partitioning of DNAzyme-A10 compared to the unmodified DNAzyme.

To ensure the inhibition was due to the partitioning in the droplet and not the design of the partitioning arms, we designed two similar DNAzymes with single A20 arms on either the 5' or 3' end. Our results confirmed that the design of the partitioning arms had no noticeable impact on the activity (Figure S10). This indicates that all modified DNAzymes were inhibited by the droplets. We also monitored the pH throughout the reaction and found a maximum transient increase of 0.04, which should not affect the folding or the activity of the DNAzyme (Supporting Table S5).

To understand the effect of each droplet component on the modified DNAzyme's activity, we compared the reaction yield after 60 minutes in the presence of different droplet components (Figure 2B). The fuel had no impact on the DNAzyme-A10 activity. In contrast, both the polyU and the peptide negatively affected the DNAzyme-A10 activity. Specifically, the polyU reduced the activity by 45 % and the peptide by 70 %. Combining the fuel with peptide or polyU did not further decrease the activity. When all three droplet components are together, the activity of the DNAzyme-A10 is further reduced compared to just peptide and polyU. This finding indicates that partitioning into the droplets inhibits the activity of the modified DNAzyme. Indeed, for the unmodified DNAzyme, we found no difference between the effect of polyU and peptide and all three components (Figure S5). We did unpaired t-tests to measure the significance of all results (Figure S14).

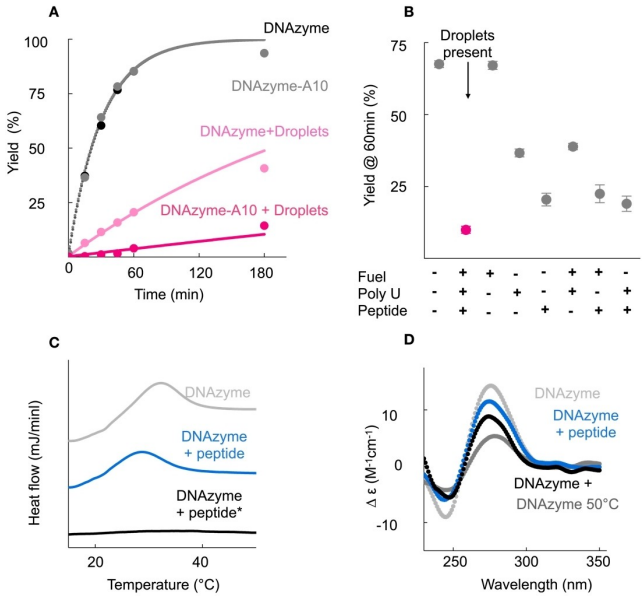

Figure 2. DNAzyme activity is inhibited inside droplets. **A**. Kinetics of DNAzyme-catalyzed reaction analyzed by PAGE (markers) over three hours. A first-order regression over the first 60 minutes was used to fit the data (line). The droplets inhibit the DNAzyme activity, which is more pronounced for DNAzyme-A10. The [DNAzyme] was 1 μM, and the [substrate] was 4 μM. The sample was fueled over the first 45 minutes with 10 mM EDC every 5 minutes. **B**. Screening of DNAzyme A10 reaction yield at 60 minutes in the presence of different droplet components analyzed by PAGE. Except for 1 μM of substrate, we used the same conditions as in A. The error bar corresponds to the standard deviation of the average of three replicates. If none are visible, they are smaller than the size of the data point. **C**. Raw heat flow against temperature as measured by DSC, using 3 mM of peptide or peptide* each with 140 μM of the unmodified DNAzyme. Peptide* is a stable mimic of the activated peptide. **D**. CD spectra of 1.6 μM unmodified DNAzyme in the presence or absence of 1 mM peptide or peptide* at 25 °C. For comparison, the spectra of the DNAzyme at 50 °C were obtained, showing thermal unfolding.

Mechanism of Inhibition

We investigated the mechanism of DNAzyme inhibition by the peptide using differential scanning calorimetry (DSC) and circular dichroism spectroscopy (CD). Specifically, we probed the stability of the folded DNAzyme in the presence and absence of both peptide (Ac-F(RG)$_3$D-OH) and a stable model of the activated peptide (Ac-F(RG)$_3$N-NH$_2$, peptide*). In peptide*, the C-terminal aspartic acid is substituted with an amidated asparagine, and thus, it mimics the three positive charges of the anhydride without its transient nature. Experiments with peptide* did not contain any fuel. In the DSC measurement, we used 140 μM of DNAzyme and 3 mM of peptide or peptide* to obtain a detectable signal. Without the peptide, we observed a transition at 31.5 °C, indicating the DNAzyme's unfolding (Figure 2C). With the peptide, the transition peak broadened, and its maximum shifted to 28.7 °C. Moreover, we measured a decrease in the calorimetric enthalpy from 238 to 201 kJ/mol K (Figure S6). Both observations confirm the peptide destabilizes the DNAzyme even at concentrations below the experimental conditions. In the presence of 3 mM of peptide*, mimicking the concentration of activated peptide around 5 minutes into the cycle (See Supporting Note 1), the transition disappeared completely, implying

© 2024 The Authors. Angewandte Chemie International Edition published by Wiley-VCH GmbH

15213773, 2024, 47, Downloaded from https://onlinelibrary.wiley.com/doi/10.1002/anie.202412534, Wiley Online Library on [14/11/2024]. See the Terms and Conditions (https://onlinelibrary.wiley.com/terms-and-conditions) on Wiley Online Library for rules of use; OA articles are governed by the applicable Creative Commons License

that almost none of the DNAzyme was in the catalytically active folded state (Figure 2C).

Next, we explored the impact of the peptides on DNAzyme folding using CD spectroscopy. We used 1.6 μM of DNAzyme for the CD spectra and 0.05 to 1 mM of peptide and peptide*. For samples containing 1 mM peptide and peptide*, we observe a decreased amplitude of the circular dichroism signal similar to a thermal unfolding of the hairpin structure of the DNAzyme (Figure 2D). In a titration series, we found a dose-dependency of the unfolding to the peptide concentrations (Figure S12). As observed for the DSC measurements, peptide* impacted the unfolding characteristics of the DNAzyme to a much larger extent than the peptide (Figure S12). This finding was further confirmed by repeating the activity measurements from Figure 2A with 2.5 mM peptide* and 2.5 mM peptide (Figure S13), demonstrating significantly stronger inhibition with peptide*.

These combined experiments show that the DNAzyme's activity is inhibited because both peptide and peptide* unfold its catalytically active conformation. Since the concentration of peptides and DNAzyme in the droplets is substantially higher than in solution, we assume the inhibitory effect is enhanced in the droplet environment, leading to complete inhibition of the DNAzyme population inside the complex coacervates.

Droplets Spatiotemporally Control Dnazyme Activity

Excited by the ability of our droplets to regulate the DNAzyme-A10 activity, we speculated we could temporally control the activity of the DNAzyme-A10 by utilizing the transient nature of the droplets (Figure 3A). We used the kinetic model to predict the time-dependent activated peptide concentration after fuel addition. Based on the CD data above, we set 0.1 mM activated peptide as a threshold above which we expected most DNAzyme-A10 to be inhibited by the droplets (Figure 3A). We found that a single batch of 40 mM EDC sustained the activated peptide concentration above this threshold for 22 minutes. Confocal microscopy confirmed the fuel-induced droplet formation, the dissolution of the majority of droplets, and the release of most of DNAzyme-A10 after the threshold had been reached (Figure 3B). We quantified the progress of the reaction for the DNAzyme-A10 by following the product formation by PAGE after adding 40 mM fuel (Figure 3C). In the first 15 minutes, i.e., well above the threshold of activated peptide, we found 1 % of substrate conversion. The conversion had increased drastically in the following 15 minutes as an additional 2.5 % substrate was converted. That increased conversion rate was sustained for the following time points. In other words, the presence of the droplets inhibited DNAzyme-A10 2.5-fold, which was recovered when most fuel was depleted.

We repeated the experiment by refueling the sample after 60 and 120 minutes. As before, DNAzyme-A10 activity was drastically inhibited 15 minutes after fuel addition and mostly recovered afterward. We hypothesize that the

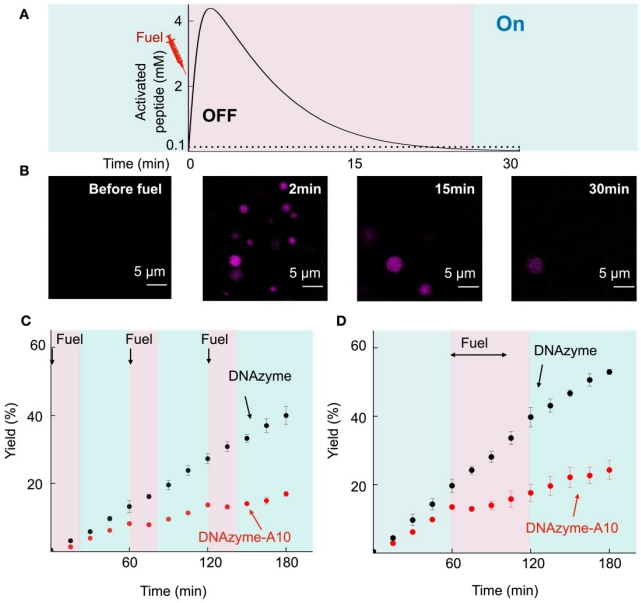

Figure 3. DNAzyme activity is spatiotemporally controlled by active droplets. **A**. Activated peptide concentration after the addition of 40 mM fuel predicted by the kinetic model. 0.1 mM was set as a minimum threshold for inhibition. **B**. Confocal micrographs of active droplets containing 200 nM Cy3-tagged DNAzyme-A10. The micrographs were acquired before and 5, 15, and 30 minutes after fuel addition. The color-coding correlates to the DNAzyme-A10 concentration. The majority of droplets dissolve in 30 minutes. **C**–**D**. The yields of the DNAzyme catalyzed reaction against time as measured by PAGE. Over 180 minutes, we fueled either three times every 60 minutes with 40 mM (**C**) or nine small 10 mM doses every 5 minutes starting one hour into the reaction (**D**). The period when the activated peptide is predicted to exceed the threshold is shaded purple. The error bars represent the standard deviation of the average of three replicates; if none are visible, they are smaller than the data point.

incomplete activity recovery is due to the zinc-induced persistence of the remaining droplets. To confirm this hypothesis, we measured the activity of both DNAzymes after complete droplet dissolution, adding the $ZnCl_2$ and starting the reaction 30 minutes after fuel addition. We found no difference in the experiment with prior fuel addition compared to the ones without, confirming that incomplete DNAzyme-A10 activity recovery is due to incomplete dissolution of droplets in the presence of $ZnCl_2$ (Figure S11).

Excitingly, when we repeated the refueling experiment with the unmodified DNAzyme, i.e., the DNAzyme lacking the A_{10} arms, the fuel-induced droplet formation had no effect. In other words, by adding partitioning arms, we can control whether or not the active droplets affect certain reaction pathways.

Next, we sustained the inhibition of DNAzyme activity by creating a steady state of the activated peptide. We did so by adding 10 mM shots of fuel every 5 minutes (Figure 3D, Figure S7). After monitoring the DNAzyme-catalyzed reaction for 60 minutes, we created a steady state of activated peptide for the next 60 minutes. The kinetic model predicted that the activated peptide concentration exceeded the

© 2024 The Authors. Angewandte Chemie International Edition published by Wiley-VCH GmbH

15213773, 2024, 47, Downloaded from https://onlinelibrary.wiley.com/doi/10.1002/anie.202412534, Wiley Online Library on [14/11/2024]. See the Terms and Conditions (https://onlinelibrary.wiley.com/terms-and-conditions) on Wiley Online Library for rules of use; OA articles are governed by the applicable Creative Commons License

threshold value immediately and was sustained for 60 minutes. Again, the unmodified DNAzyme did not change its reaction rate after the formation of droplets. In contrast, substrate conversion by DNAzyme-A10 was strongly inhibited right after fuel addition. The DNAzyme-A10 activity slowly recovered after 30 minutes, earlier than the kinetic model predicted. We believe this to be most likely due to exhaustion of the system and accumulation of waste after extensive fuelling. Moreover, the activity of DNAzme-A10 again did not fully recover to the initial state before the fuel was added. Taken together, we can briefly pause DNAzyme activity or sustain it for longer periods.

Conclusion

We demonstrated that active droplets regulate the activity of a DNAzyme spatiotemporally. The microenvironment of the active droplets unfolds the DNAzyme, thereby inhibiting its catalytic activity. By modifying the DNAzyme with two A10 arms, we increased the partitioning of the catalyst into the droplets, enabling us to control its activity. Given the transient nature of the droplets, the inhibition is temporary and can be modulated by the fuelling pattern.

In biology, chemical reaction networks are constantly up and downregulated. Recent findings show that sequestration inside membraneless organelles is important in this regulation.[18a,1b,18b] We foresee that combining DNAzymes with active droplets can up or downregulate multiple reactions in a network, thereby emulating the complexity of a cell's biological pathways. These reaction networks, especially where the DNAzyme reciprocally regulates the droplet properties, are a powerful model for understanding better regulation in the cell. It will also be a powerful tool for synthetic biology and synthetic cell research.

Supporting Information

The authors have cited additional references within the Supporting Information.[9a,16]

Acknowledgements

The BoekhovenLab is grateful for support from the TUM Innovation Network—RISE funded through the Excellence Strategy. This research was conducted within the Max Planck School Matter to Life, supported by the German Federal Ministry of Education and Research (BMBF) in collaboration with the Max Planck Society. The work was funded by the Deutsche Forschungsgemeinschaft (DFG, German Research Foundation) under Germany's Excellence Strategy - EXC-2094—390783311 and the European Research Council, ERC (JB) and 802000 (HM). Open Access funding enabled and organized by Projekt DEAL.

Conflict of Interest

The authors declare no conflict of interest.

Data Availability Statement

The data that support the findings of this study are available from the corresponding author upon reasonable request.

Keywords: DNAzyme · Artificial Organelles · Transient catalysis · Coacervates · Synthetic Biology

[1] a) C. P. Brangwynne, C. R. Eckmann, D. S. Courson, A. Rybarska, C. Hoege, J. Gharakhani, F. Jülicher, A. A. Hyman, *Sci. J.* **2009**, *324*, 1729–1732; b) S. F. Banani, H. O. Lee, A. A. Hyman, M. K. Rosen, *Nat. Rev. Mol. Cell Biol.* **2017**, *18*, 285–298; c) J. B. Woodruff, A. A. Hyman, E. Boke, *Trends Biochem. Sci.* **2018**, *43*, 81–94; d) E. Gomes, J. Shorter, *J. Biol. Chem.* **2019**, *294*, 7115–7127; e) T. Yoshizawa, R.-S. Nozawa, T. Z. Jia, T. Saio, E. Mori, *Biophys. Rev. Lett.* **2020**, *12*, 519–539; f) T. Hirose, K. Ninomiya, S. Nakagawa, T. Yamazaki, *Nat. Rev. Mol. Cell Biol.* **2023**, *24*, 288–304.

[2] a) W. M. Aumiller, Jr., F. Pir Cakmak, B. W. Davis, C. D. Keating, *Langmuir* **2016**, *32*, 10042–10053; b) A. J. Plys, R. E. Kingston, *Sci. J.* **2018**, *361*, 329–330.

[3] a) S. Koga, D. S. Williams, A. W. Perriman, S. Mann, *Nat. Chem.* **2011**, *3*, 720–724; b) V. N. Uversky, I. M. Kuznetsova, K. K. Turoverov, B. Zaslavsky, *FEBS Lett.* **2015**, *589*, 15–22; c) A. S. Holehouse, B. B. Kragelund, *Nat. Rev. Mol. Cell Biol.* **2023**.

[4] a) J. Uniacke, W. Zerges, *J. Cell Biol.* **2008**, *182*, 641–646; b) P. Anderson, N. Kedersha, *Curr. Biol.* **2009**, *19*, R397–R398; c) D. S. W. Protter, R. Parker, *Trends Cell Biol.* **2016**, *26*, 668–679.

[5] a) C. E. Sing, S. L. Perry, *Soft Matter* **2020**, *16*, 2885–2914; b) M. Abbas, W. P. Lipiński, J. Wang, E. Spruijt, *Chem. Soc. Rev.* **2021**, *50*, 3690–3705.

[6] a) R. R. Poudyal, R. M. Guth-Metzler, A. J. Veenis, E. A. Frankel, C. D. Keating, P. C. Bevilacqua, *Nat. Commun.* **2019**, *10*, 490; b) A. Testa, M. Dindo, A. A. Rebane, B. Nasouri, R. W. Style, R. Golestanian, E. R. Dufresne, P. Laurino, *Nat. Commun.* **2021**, *12*, 6293; c) W. A. Wee, H. Sugiyama, S. Park, *iScience* **2021**, *24*, 103455; d) L. Zhou, Y. Fan, Z. Liu, L. Chen, E. Spruijt, Y. Wang, *CCS Chem.* **2021**, *3*, 358–366; e) T. Komachi, S. Kawai, Y. Hirayama, A. Maruyama, N. Shimada, *Polym. Chem.* **2023**, *14*, 4743–4747; f) K. K. Le Vay, E. Salibi, B. Ghosh, T. Y. D. Tang, H. Mutschler, *eLife* **2023**, *12*, e83543; g) J. Wang, M. Abbas, J. Wang, E. Spruijt, *Nat. Commun.* **2023**, *14*, 8492.

[7] a) S. Tagami, J. Attwater, P. Holliger, *Nat. Chem.* **2017**, *9*, 325–332; b) R. R. Poudyal, C. D. Keating, P. C. Bevilacqua, *ACS Chem. Biol.* **2019**, *14*, 1243–1248.

[8] A. K. Rai, J.-X. Chen, M. Selbach, L. Pelkmans, *Nature* **2018**, *559*, 211–216.

[9] a) C. Donau, F. Späth, M. Sosson, B. A. K. Kriebisch, F. Schnitter, M. Tena-Solsona, H.-S. Kang, E. Salibi, M. Sattler, H. Mutschler, J. Boekhoven, *Nat. Commun.* **2020**, *11*, 5167; b) F. Späth, C. Donau, A. M. Bergmann, M. Kränzlein, C. V. Synatschke, B. Rieger, J. Boekhoven, *J. Am. Chem. Soc.* **2021**, *143*, 4782–4789; c) C. Donau, F. Späth, M. Stasi, A. M. Bergmann, J. Boekhoven, *Angew. Chem. Int. Ed.* **2022**, *61*, e202211905; d) A. M. Bergmann, J. Bauermann, G. Bartolucci, C. Donau, M. Stasi, A.-L. Holtmannspötter, F. Jülicher, C. A.

© 2024 The Authors. Angewandte Chemie International Edition published by Wiley-VCH GmbH

15213773, 2024, 47, Downloaded from https://onlinelibrary.wiley.com/doi/10.1002/anie.202412534, Wiley Online Library on [14/11/2024]. See the Terms and Conditions (https://onlinelibrary.wiley.com/terms-and-conditions) on Wiley Online Library for rules of use; OA articles are governed by the applicable Creative Commons License

Weber, J. Boekhoven, *Nat. Commun.* **2023**, *14*, 6552; e) F. Späth, A. S. Maier, M. Stasi, A. M. Bergmann, K. Halama, M. Wenisch, B. Rieger, J. Boekhoven, *Angew. Chem. Int. Ed.* **2023**, *62*, e202309318; f) S. M. Poprawa, M. Stasi, B. A. K. Kriebisch, M. Wenisch, J. Sastre, J. Boekhoven, *Nat. Commun.* **2024**, *15*, 4204.

[10] a) W. M. Aumiller, C. D. Keating, *Nat. Chem.* **2016**, *8*, 129–137; b) G. Cheng, J. Perez-Mercader, *Chem* **2020**, *6*, 1160–1171; c) C. Donau, J. Boekhoven, *Trends Chem.* **2023**, *5*, 45–60.

[11] a) K. Das, L. Gabrielli, L. J. Prins, *Angew. Chem. Int. Ed.* **2021**, *60*, 20120–20143; b) X. Chen, M. A. Würbser, J. Boekhoven, *Accounts of Materials Research* **2023**, *4*, 416–426.

[12] M. A. Würbser, P. S. Schwarz, J. Heckel, A. M. Bergmann, A. Walther, J. Boekhoven, *ChemSystemsChem* **2021**, *3*, e2100015.

[13] a) M. A. Cardona, L. J. Prins, *Chem. Sci.* **2020**, *11*, 1518–1522; b) R. Chen, S. Neri, L. J. Prins, *Nat. Nanotechnol.* **2020**, *15*, 868–874.

[14] a) R. R. Breaker, G. F. Joyce, *Chem. Biol.* **1994**, *1*, 223–229; b) B. Cuenoud, J. W. Szostak, *Nature* **1995**, *375*, 611–614; c) E. Golub, R. Freeman, I. Willner, *Angew. Chem. Int. Ed.* **2011**, *50*, 11710–11714.

[15] G. F. Joyce, *Annu. Rev. Biochem.* **2004**, *73*, 791–836.

[16] M. Tena-Solsona, B. Rieß, R. K. Grötsch, F. C. Löhrer, C. Wanzke, B. Käsdorf, A. R. Bausch, P. Müller-Buschbaum, O. Lieleg, J. Boekhoven, *Nat. Commun.* **2017**, *8*, 15895.

[17] a) J. Li, Y. Lu, *J. Am. Chem. Soc.* **2000**, *122*, 10466–10467; b) A. K. Brown, J. Li, C. M. B. Pavot, Y. Lu, *Biochem.* **2003**, *42*, 7152–7161.

[18] a) S. Alberti, *J. Cell Sci.* **2017**, *130*, 2789–2796; b) Y. Shin, C. P. Brangwynne, *Sci. J.* **2017**, *357*, eaaf4382.

Manuscript received: July 3, 2024
Accepted manuscript online: August 9, 2024
Version of record online: October 15, 2024

© 2024 The Authors. Angewandte Chemie International Edition published by Wiley-VCH GmbH

15213773, 2024, 47, Downloaded from https://onlinelibrary.wiley.com/doi/10.1002/anie.202412534, Wiley Online Library on [14/11/2024]. See the Terms and Conditions (https://onlinelibrary.wiley.com/terms-and-conditions) on Wiley Online Library for rules of use; OA articles are governed by the applicable Creative Commons License